Applications of Image Filtration Based on Principal Component Analysis and Nonlocal Image Processing

Andrey Priorov, Kirill Tumanov, *Member, IAENG and Student Member, IEEE,* Vladimir Volokhov, Evgeny Sergeev and Ivan Mochalov

***Abstract*— Number of works covers a topic of denoising of digital images affected by an additive white Gaussian noise (AWGN), which are formed by typical devices that contain of lenses and semiconducting sensors which capture a projected scene. These constructive elements inevitably add numerous distortions, degradation and noise. Some tasks require high-quality digital images, this leads to the development of denoising algorithms which also sharpen an image and perform its colour correction. In this paper we present our results of applying several image filtration algorithms based on Principal Component Analysis (PCA) and non-local processing. Work is focused on a discussion of experimental data which is aimed to uncover best practices of use for the studied filtration algorithms.**

***Index Terms*—Image filtration, principal component analysis, non-local processing, applications**

I. Introduction

As it was shown by Chatterjee and Milanfar in 2010, the theoretical limit of image reconstruction hasn't been yet achieved [1]. There still are debates on how to increase performance of filtration techniques used today. Among the widest spread methods of cancelling an AWGN in digital images, according to [2], are the algorithms which base on: (1) local processing, (2) non-local processing, (3) pointwise processing and (4) multipoint processing.

All the named methods evolved through the years and now each of them has sophisticated implementations which compete with each other on the test metrics. That is why most of researchers consider their own evaluations of image reconstruction for specific textural, edge and contrast regions. The main problems with the quality of reconstructed images which researches try to evaluate are: a Gibbs effect, which becomes highly noticeable on images containing objects with high brightness contrast on their outer edges, and an edge blurring of objects on an image being processed. Both of these effects highly degrade an image perception and could not be suited for high demands.

List of the most successful solutions to the stated problems includes the following digital image reconstruction algorithms: (1) algorithm based on block-matching and 3D filtering (BM3D) [3]; (2) algorithm based on shape-adaptive discrete cosine transform (SA-DCT) [4]; (3) k-means singular value decomposition (K-SVD) [5]; (4) non-local means algorithm (NL-means) [6]; (5) algorithm based on a local polynomial approximation and intersection of confidence intervals rule (LPA-ICI) [7].

In our previous work [8], we proposed a parallel filtration scheme algorithm based on PCA and non-local processing. In the present study we compare sequential and parallel filtration schemes in terms of their work principles and the results of their use in modern digital image filtration tasks.

Literature on digital images noise cancelling shows that modern AWGN filtration methods used for greyscale images may be successfully transferred to other digital image processing tasks. So, this work in addition to the primary use of the methods shows how they may be used for: (1) denoising AWGN-affected colour images; (2) filtration of mixed noises from greyscale images; (3) suppression of blocking artefacts in compressed JPEG images; (4) filtration of mixed noises from colour images.

Usage of the AWGN model may be explained with the help of statistics theory, namely – central limit theorem. It has an important practical value and is suitable for describing the work of devices containing numerous independent additive noise sources, each of which has its own random distribution, which may be unknown. Resulting sum of these noise distributions is best described as a Gaussian distribution. On practice AWGN model well suits to simulate a thermal noise which is inevitably observed in digital devices such as charge-coupled devices (CCDs) or CMOS matrixes.

Filtration of colour images is an issue of the day for various practical applications. That is why there are numerous solutions to it. As a possible approach, in this work we did no transition from RGB image to an image with separated brightness and colour information, and added an AWGN separately to each channel with the same characteristics. This method was used for simplicity and for further research it may be extended by using specific noise models and applying them to each image layer in a variation of interest.

This work was supported in part by the Russian Foundation for Basic Research under Grant № 12-08-01215-a "Development of methods for quality assessment of video".

A.L. Priorov is with the Yaroslavl State University, Yaroslavl, Russia 150000 (e-mail: andcat@yandex.ru).

K.I. Tumanov is with the Yaroslavl State University, Yaroslavl, Russia 150000 (corresponding author, phone: +7-910-814-2226; e-mail: tumanov@susqu.edu).

V.A. Volokhov is with the Yaroslavl State University, Yaroslavl, Russia 150000 (e-mail: volokhov@piclab.ru).

E.V. Sergeev is with the Yaroslavl State University, Yaroslavl, Russia 150000 (e-mail: sergeev@piclab.ru).

I.S. Mochalov is with the Yaroslavl State University, Yaroslavl, Russia 150000 (e-mail: yar_panda@yahoo.com).

(Advance online publication: 21 May 2013)

II. Used filtration schemes description

For the present study we took two similar methods which both used PCA and non-local means approaches.

A. *Two-stage PCA filtration scheme*

Both sequential and parallel filtration schemes used the modification of two-stage PCA filtration scheme (Adaptive PCA + empiric Wiener filter (APCA+Wiener for short)).

Conceptual structure of two-stage PCA filtration procedure is given in Fig. 1. It can be observed that the first processing stage forms a first "raw" evaluation $\hat{\mathbf{x}}^{\mathrm{I}}$ of an unnoised image $\mathbf{x}$. After that, on the second processing stage, a "fine" evaluation $\hat{\mathbf{x}}^{\mathrm{II}}$ of an unnoised image $\mathbf{x}$ is formed based on the "raw" evaluation $\hat{\mathbf{x}}^{\mathrm{I}}$, received after the previous stage.

We decided to test this filtration scheme along with two more advanced ones in order to see, how the latter two perform in comparison with the APCA+Wiener, which is one of their major components.

B. *Sequential filtration scheme*

Next method is a sequential filtration scheme shown on Fig. 2. First, as it was noted, this scheme includes an abovementioned APCA+Wiener filtration scheme as a base which forms an input for non-local denoising algorithm. The latter algorithm calculates the non-local means discussed previously [6, 9-11]. As a result we receive a final non-local evaluation of the processed pixel $\hat{\mathbf{x}}^{\mathrm{II}}(i, j)$ using the following formula:

$$\hat{x}^{\mathrm{III}}(i, j) = \sum_{k,l} g_{h^{\mathrm{III}}}(i, j, k, l)\hat{\mathbf{x}}^{\mathrm{II}}(k, l), \quad (1)$$

where $g_{h^{\mathrm{III}}}(i, j, k, l) = \dfrac{w_{h^{\mathrm{III}}}(i, j, k, l)}{\sum_{k,l} w_{h^{\mathrm{III}}}(i, j, k, l)}$ (2).

C. *Parallel filtration scheme*

The last method used in this work, and discussed in detail [8], is a parallel filtration scheme based on the same algorithms which were used in the previous method. Scheme of the parallel filtration is shown in Fig. 3.

Notable is that the "Two-stage PCA based filtration" block performs completely same tasks that it does in a sequential scheme. On the other hand, contrary to the previous method, block "Non-local algorithm of image denoising" processes a noised image $\mathbf{y}$, not a second evaluation $\hat{\mathbf{x}}^{\mathrm{II}}$ of an unnoised image $\mathbf{x}$ (This is marked with an arrow from the "Two-stage PCA based filtration" block to the block of "Non-local algorithm of image denoising" on the Fig. 3). Wherein weight of a pixel $y(k, l)$ similar to a processed pixel $y(i, j)$ in a final evaluation $\hat{\mathbf{x}}^{\mathrm{III}}$ of an unnoised image $\mathbf{x}$, received as an output of the block, is calculated using the formula:

$$w_{h^{\mathrm{III}}}(i, j, k, l) = e^{-\frac{\sum_{m,n\in N} g_a(m,n)\cdot[\hat{x}^{\mathrm{II}}(i+m, j+n) - \hat{x}^{\mathrm{II}}(k+m, l+n)]^2}{(h^{\mathrm{III}})^2}}. \quad (3)$$

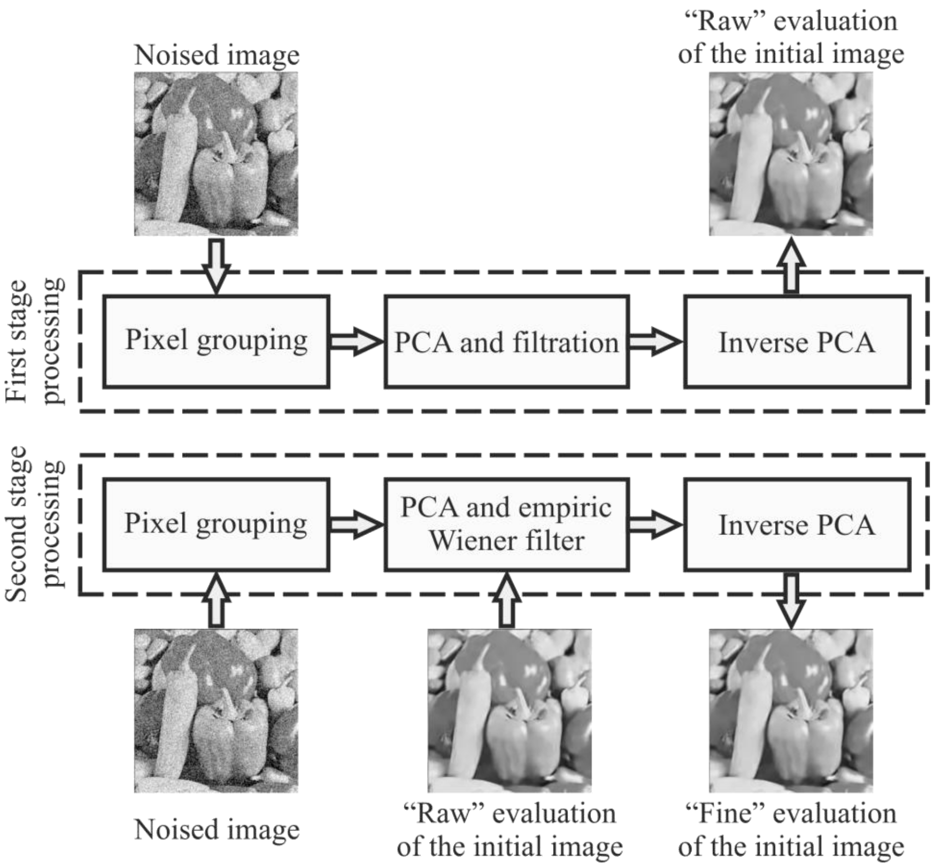

Fig. 1. Two-stage PCA-based filtration scheme

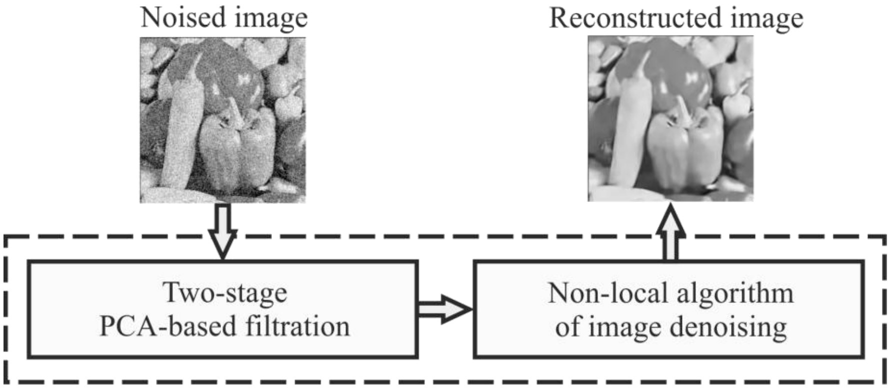

Fig. 2. Sequential digital image filtration scheme

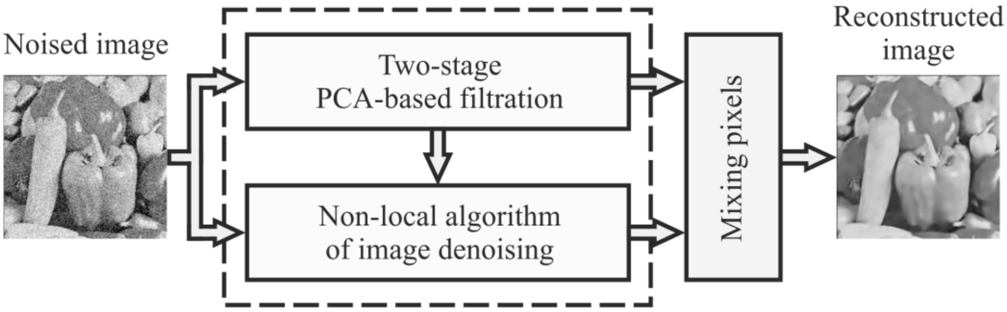

Fig. 3. Parallel digital image filtration scheme

Based on the foregoing, the final non-local evaluation of the processed pixel $y(i,j)$ is formed basing on the following:

$$\hat{x}^{\mathrm{III}}(i,j)=\sum\nolimits_{k,l} g_{h^{\mathrm{III}}}(i,j,k,l)y(k,l), \quad (4)$$

where $g_{h^{\mathrm{III}}}(i,j,k,l)$ is calculated using formula (2), and weights $w_{h^{\mathrm{III}}}(i,j,k,l)$ may be found using expression (3).

In addition, parallel scheme uses a supplemental “Mixing pixels” block which forms a final “accurate” evaluation $\hat{\mathbf{x}}^{\mathrm{IV}}$ of an unnoised image $\mathbf{x}$.

In the present work mixing pixels procedure was implemented using the following simple formula:

$$\hat{\mathbf{x}}^{\mathrm{IV}}=d^{\mathrm{II}}\cdot\hat{\mathbf{x}}^{\mathrm{II}}+d^{\mathrm{III}}\cdot\hat{\mathbf{x}}^{\mathrm{III}}, \quad (5)$$

where d^{II} and d^{III} – are constants with values less than 1.

III. Methods’ applicability for AWGN-affected greyscale image filtration

In our work values of constants c^{III} were selected empirically and the results of AWGN-affected greyscale image filtration for a sequential filtration scheme are given in Table 1. Specific values of Peak Signal-to-Noise Ratio (PSNR) and Mean Structural Similarity Index Map (MSSIM) are shown for each algorithm. Hereinafter best image reconstruction results based on the criteria of PSNR [12] and MSSIM [13] are marked in bold. Experimental results are shown for 10 greyscale images from [14] with σ values in a range from 5 to 35 and for c^{III} – from 0.2 to 0.5. It can be concluded that best results are obtained with c^{III} equal to 0.3. MSSIM quality assessment shows that the use of the third processing stage in the sequential filtration scheme is rational for noise with $\sigma\geq 20$. Results analysis shows that the further increase of c^{III} leads to an excessive decrease of ringing artefacts on a foreground edges. In addition, while the c^{III} value is increasing same happens to h^{III} value, and thus an image resulting from a second stage processing is additionally smoothed, which in turn gradually decreases a reconstructed image quality.

Notable is that the use of the sequential filtration scheme allows only to remove ringing artefacts from the main objects’ edges, but the decrease of a blurring effect is not observed. The latter is connected with the structure of the third processing stage. A preliminary filtered image from the second processing stage, which already contains traces of the blurring on its objects’ edges, comes as an input to the non-local filtration algorithm. The overcome of this limitation is implemented in a parallel filtration scheme.

Results of a same set of AWGN-affected greyscale images filtration for a parallel filtration scheme are given in Table 2. Comparing Tables 1 and 2 based on PSNR and MSSIM metrics it can be concluded that the use of the third and fourth processing stages is rational for $\sigma\geq 15$.

The use of parallel filtration scheme allows both to remove ringing artefacts and blurring effect from the objects’ edges. It may be explained by the fact that a noised image $\mathbf{y}$ is used as an input to the “Two-stage PCA based filtration” block and to the block of “Non-local algorithm of image denoising”, shown on the Fig. 3. This allows to have two independent evaluations of an unnoised image $\mathbf{x}$, in one of which, namely received from the “Two-stage PCA based filtration” block, texture specifics of an unnoised image $\mathbf{X}$ are better preserved, and in the second - “Non-local algorithm of image denoising”, the main objects’ edges are better preserved. Union of these two evaluations using an equation (5) allows forming of a higher quality evaluation of an unnoised image $\mathbf{x}$.

TABLE 1
Results of quality assessment of greyscale digital image filtration using a sequential filtration scheme

Number of processing stages		1	2	3			
				c^{III} value			
				0.2	0.3	0.4	0.5
Average PSNR and MSSM results for 10 test images							
PSNR, dB	σ = 5	37.78	**38.02**	36.65	36.19	35.99	35.90
	σ = 15	31.79	**32.29**	31.97	31.97	32.00	32.00
	σ = 20	30.29	**30.86**	30.70	30.73	30.74	30.74
	σ = 25	29.12	**29.75**	29.68	29.70	29.71	29.69
	σ = 35	27.34	27.99	27.99	**28.00**	27.97	27.92
MSSM	σ = 5	0.949	**0.953**	0.943	0.941	0.941	0.940
	σ = 15	0.855	**0.879**	0.876	0.876	0.876	0.875
	σ = 20	0.814	**0.851**	0.850	**0.851**	0.850	0.848
	σ = 25	0.777	0.825	**0.827**	**0.827**	0.826	0.824
	σ = 35	0.714	0.781	**0.785**	**0.785**	0.782	0.779

Specific numerical results of AWGN-affected greyscale digital images filtration with sequential and parallel filtration schemes are given for images size of 256×256 pixels and 512×512 pixels in Table 3 and Table 4 respectfully. Their analysis helps to conclude that the use of: (1) sequential filtration scheme does not give an increase in reconstructed image quality assessed with PSNR and MSSIM, however, with low c^{III} values this scheme allows to remove the ringing artefacts; (2) parallel scheme increases a reconstructed image quality along with the removal of ringing artefacts and reducing the blurring effect on the object's edges.

Overall the quality of a reconstructed image is comparable with the BM3D algorithm which provides best quality of a reconstructed image among the overviewed filtration algorithms. The average loss of the parallel scheme in comparison with BM3D is for PSNR ~ 0.53 dB and ~ 0.008 for MSSIM. While the perceptional quality of reconstructed images filtered by the parallel scheme is high and very close to the one obtained by BM3D [3].

Results of AWGN-affected greyscale digital images filtration with sequential and parallel filtration schemes are visualised on Fig. 4 on an examples of "Boat" size of 512×512 pixels and "Barbara" size of 256×256 pixels images.

IV. Usage of the Filtration Schemes in Modern Image Processing Tasks

Modern AWGN filtration methods applied to greyscale images may be additionally used in a series of other digital image processing tasks. Examples of such tasks are: colour image filtration, filtration of "raw" images, deletion of blurring from objects' edges, sharpening of objects' edges and so on. In the present article we studied the work of APCA+Wiener, sequential and parallel filtration schemes on the tasks of: colour images filtration, mixed noise filtration from greyscale and colour images and removal of blocking artefacts.

In this section we applied APCA+Wiener, sequential and parallel filtration schemes' algorithms implemented in MATLAB to the mentioned digital image processing tasks.

A. Removal of blocking artefacts

The task was formulated as a situation where an image compression using JPEG algorithm is used as a noise model [15-16]. In this case a noise component $\mathbf{n}$ may be treated as a result of distortion connected with blocking artefacts on a digital image. Then a solution to this task may be found as dispersion σ^2 of a noise component $\mathbf{n}$. A possible way of finding σ^2, using an *a priori* knowledge about a quantization matrix of JPEG standard coefficients, is shown in [4]. In this study search of σ^2 was performed manually.

For our experiments on blocking artefacts removal we used the same source of greyscale images [14]. We tested our algorithms on 256×256 pixels and 512×512 pixels images.

TABLE 2
Results of quality assessment of greyscale digital image filtration using a parallel filtration scheme

Number of processing stages		3				4			
		c^{III} value				c^{III} value			
		0.2	0.3	0.4	0.5	0.2	0.3	0.4	0.5
Average PSNR and MSSM results for 10 test images									
PSNR, dB	σ = 5	35.56	35.64	35.73	35.81	37.41	37.45	37.48	**37.52**
	σ = 15	30.99	31.73	32.07	32.13	32.22	32.49	32.60	**32.61**
	σ = 20	29.90	30.70	30.97	30.91	30.96	31.23	**31.29**	31.25
	σ = 25	29.13	29.90	30.04	29.85	29.99	**30.22**	**30.22**	30.12
	σ = 35	28.03	28.50	28.34	27.97	28.46	**28.54**	28.42	28.24
MSSM	σ = 5	0.935	0.940	0.941	0.941	0.949	**0.951**	**0.951**	**0.951**
	σ = 15	0.865	0.877	0.876	0.871	0.880	**0.884**	**0.884**	0.882
	σ = 20	0.843	0.853	0.850	0.842	0.855	**0.859**	0.857	0.855
	σ = 25	0.824	0.831	0.825	0.815	0.834	**0.836**	0.833	0.829
	σ = 35	0.791	0.791	0.780	0.766	**0.795**	0.794	0.789	0.784

TABLE 3
PSNR and MSSIM of reconstructed 256×256 pixels images received from sequential and parallel filtration schemes

Image	σ	Sequential scheme		Parallel scheme	
		PSNR, dB	MSSIM	PSNR, dB	MSSIM
Montage	5	38.61	0.976	39.57	0.977
	15	33.43	0.944	33.90	0.943
	20	31.58	0.929	32.28	0.928
	25	30.04	0.912	30.89	0.913
	35	27.39	0.877	28.40	0.881
Cameraman	5	35.28	0.943	36.75	0.954
	15	30.02	0.877	31.12	0.889
	20	28.82	0.848	29.73	0.859
	25	27.78	0.820	28.64	0.833
	35	26.06	0.775	26.95	0.790
Peppers	5	35.60	0.943	36.86	0.949
	15	31.35	0.891	32.02	0.895
	20	30.11	0.871	30.75	0.876
	25	29.10	0.854	29.75	0.858
	35	27.37	0.820	28.06	0.826
House	5	38.42	0.948	39.12	0.954
	15	33.84	0.873	34.21	0.880
	20	32.73	0.856	33.16	0.863
	25	31.85	0.845	32.34	0.852
	35	30.40	0.828	30.96	0.834

TABLE 4
PSNR and MSSIM of reconstructed 512×512 pixels images received from sequential and parallel filtration schemes

Image	σ	Sequential scheme		Parallel scheme	
		PSNR, dB	MSSIM	PSNR, dB	MSSIM
Lenna	5	37.30	0.935	38.26	0.943
	15	33.79	0.891	34.09	0.895
	20	32.67	0.874	32.94	0.878
	25	31.74	0.858	32.03	0.862
	35	30.20	0.830	30.52	0.833
Boat	5	35.10	0.918	36.44	0.934
	15	31.37	0.840	31.80	0.850
	20	30.19	0.810	30.59	0.820
	25	29.21	0.782	29.63	0.792
	35	27.61	0.730	28.02	0.741
Barbara	5	36.12	0.957	37.57	0.962
	15	32.42	0.915	32.65	0.919
	20	31.17	0.896	31.41	0.901
	25	30.09	0.875	30.39	0.881
	35	28.23	0.827	28.64	0.836
Couple	5	35.21	0.947	36.58	0.936
	15	31.07	0.867	31.64	0.855
	20	29.85	0.834	30.37	0.821
	25	28.85	0.803	29.34	0.790
	35	27.21	0.742	27.61	0.730

TABLE 5
PSNR and MSSIM of JPEG compressed 256×256 pixels images after reconstruction

Image	Q	σ	Noised image		APCA+Wiener		Sequential scheme		Parallel scheme	
			PSNR, dB	MSSIM	PSNR, dB	MSSIM	PSNR, dB	MSSIM	PSNR, dB	MSSIM
Aerial	5	15	22.32	0.672	23.19	0.710	23.20	0.709	23.08	0.707
		20			23.27	0.709	23.27	0.706	23.22	**0.711**
		25			23.26	0.703	23.22	0.694	**23.29**	0.708
	10	15	24.85	0.791	24.63	0.812	25.50	0.806	**25.64**	**0.815**
		20			25.45	0.800	25.25	0.787	25.62	0.809
		25			25.11	0.782	24.78	0.758	25.40	0.793
	15	15	26.19	0.838	26.76	0.848	26.45	0.837	**26.86**	**0.853**
		20			26.34	0.830	25.97	0.811	26.66	0.840
		25			25.79	0.806	25.29	0.775	26.23	0.818
Airplane	5	15	28.11	0.813	29.57	0.874	29.64	0.878	29.33	0.868
		20			29.81	0.881	29.95	0.888	29.69	0.881
		25			29.93	0.887	**30.16**	**0.896**	29.98	0.890
	10	15	31.54	0.861	33.16	0.914	30.32	0.920	33.27	0.917
		20			33.07	0.915	33.22	**0.921**	**33.43**	0.920
		25			32.80	0.915	32.87	0.920	33.38	**0.921**
	15	15	32.97	0.888	34.29	0.925	34.35	**0.928**	**34.53**	**0.928**
		20			33.98	0.924	33.98	0.926	34.47	**0.928**
		25			33.50	0.922	33.37	0.924	34.21	0.927

TABLE 6
PSNR and MSSIM average increase rate of JPEG compressed 256×256 pixels images after reconstruction

Q	σ	PSNR			MSSIM		
		APCA+Wiener	Sequential	Parallel	APCA+Wiener	Sequential	Parallel
5	15	3.56%	**4.22%**	3.40%	4.59%	**4.84%**	4.35%
	20	4.17%	**4.81%**	4.12%	4.78%	4.90%	**4.92%**
	25	4.49%	**5.07%**	4.69%	4.65%	4.42%	**5.00%**
10	15	3.02%	**3.44%**	3.34%	2.54%	2.39%	**2.82%**
	20	2.86%	3.07%	**3.48%**	1.88%	1.30%	**2.30%**
	25	2.33%	2.29%	**3.27%**	0.93%	-0.17%	**1.44%**
15	15	2.24%	2.39%	**2.87%**	1.06%	0.51%	**1.37%**
	20	1.54%	1.50%	**2.57%**	-0.02%	-1.06%	**0.38%**
	25	0.53%	0.21%	**1.90%**	-1.27%	-2.76%	**-0.81%**

JPEG compression quality parameter Q was used to set the degree of compression, and σ^2 varied to demonstrate a dependence of the image reconstruction quality from the filtration smoothing parameter.

Table 5 shows some numerical quality assessment results of 256×256 pixels image reconstruction on examples of “Aerial” and “Airplane” images.

Average quality increase rate of PSNR and MSSIM values of a reconstructed image compared to an input compressed image for each variable parameter tested is shown in Table 6 for each of the studied schemes.

Notable is that the average increase rate for each algorithm was relatively low both on PSNR and MSSIM scales. It also can be seen that images compressed with $Q = 15$ after the processing with each of the algorithms were more damaged than reconstructed. This sets an important benchmark for further investigations in this specific application of filtration methods.

Special attention through all our further test analysis was devoted to the best performance results for each combination of variables and an algorithms’ comparison based on this data. Table 7 illustrates the algorithms comparison by the number of best results shown. Hereinafter decimal values were used when two or more algorithms showed same results in one test and these numbers depict a proportion between their numbers of occurrences in a limited number of tests held. Table 8 gives a percentile outlook of the same data.

A final general overview of the proposed algorithms best performance results for this set of images is given in Table 9. From this table can be seen that best results on average show a positive dynamics of processing regardless of the negative average increase rates shown in Table 6 and discussed above. However the tempo of differential decrease in MSSIM values is much higher than the one in PSNR. This may be easily observed from the Fig. 5.

Same tests were performed with 512×512 pixels images. Similarly, numerical PSNR and MSSIM quality assessment results of reconstructed images are given in Table 10 on examples of “Bridge” and “Barbara” images. Average quality increase rate of PSNR and MSSIM values of a reconstructed image compared to an input compressed image for each variable parameter tested is shown in Table 11 for each of the studied schemes. Table 12 illustrates the algorithms comparison by the number of best results shown. Table 13 again gives a percentile outlook of the same data.

A final general overview of the proposed algorithms best performance results for this set of images is given in Table 14 and visualised in Fig. 6. Compared to Fig. 5 it can be seen, that the MSSIM decrease becomes more exponential and PSNR decreases linearly with the Q growth.

TABLE 7
Algorithms comparison by the number of best results shown
(for JPEG compressed 256×256 pixels images)

Parameter	Q	APCA+Wiener	Sequential	Parallel
PSNR	5	1.00	4.00	2.00
MSSIM		2.00	3.33	1.67
PSNR	10	0.00	1.00	6.00
MSSIM		0.00	2.69	4.31
PSNR	15	0.00	1.00	6.00
MSSIM		1.00	2.25	3.75
Total		4.00	14.28	23.72
Total # tests		42		

TABLE 8
Algorithms comparison by the percentage of best results shown
(for JPEG compressed 256×256 pixels)

Parameter	Total # tests	APCA+Wiener	Sequential	Parallel
PSNR	21	4.76%	28.57%	66.67%
MSSIM	21	14.29%	39.41%	46.31%
Average		9.52%	33.99%	56.49%

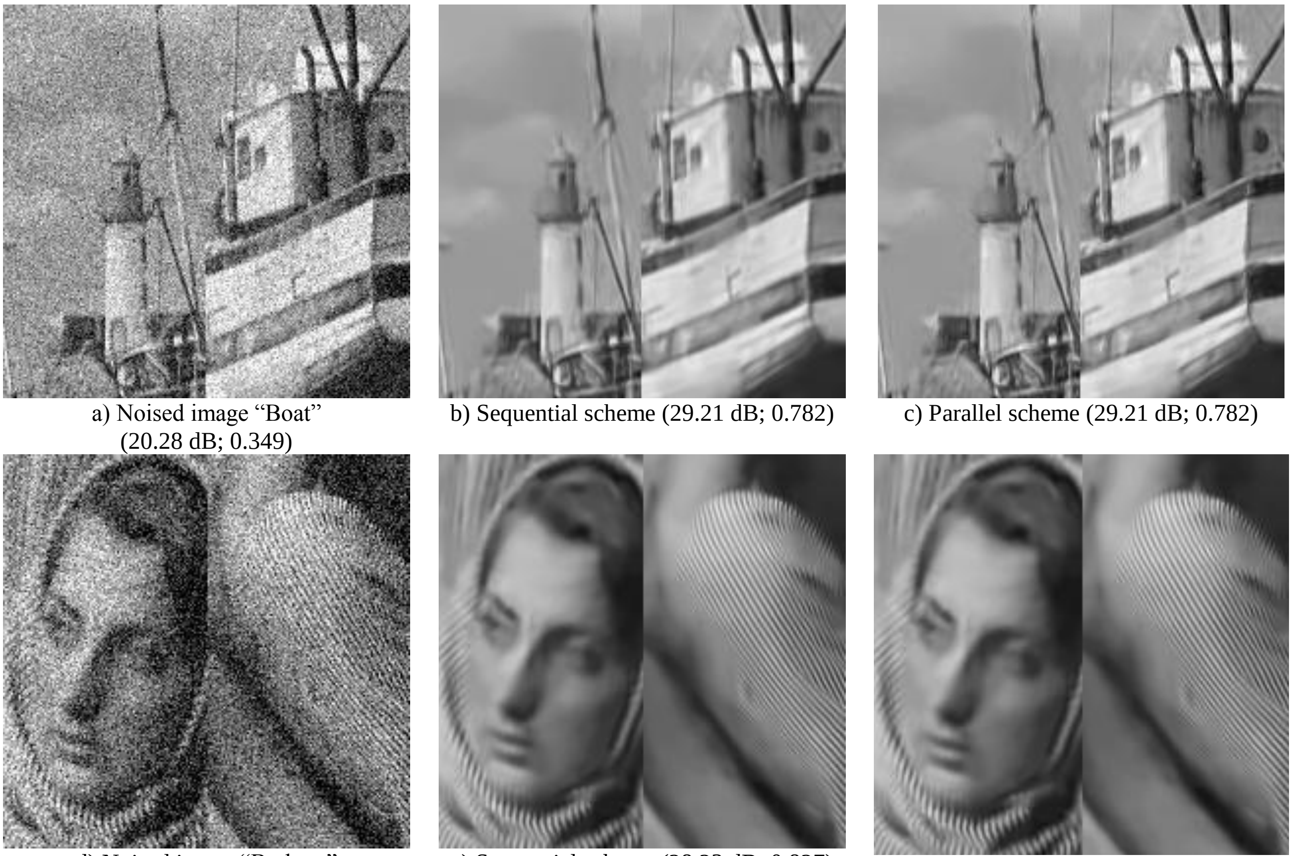

a) Noised image “Boat” (20.28 dB; 0.349)
b) Sequential scheme (29.21 dB; 0.782)
c) Parallel scheme (29.21 dB; 0.782)
d) Noised image “Barbara” (17.54 dB; 0.300)
e) Sequential scheme (28.23 dB; 0.827)
f) Parallel scheme (28.64 dB; 0.836)

Fig. 4. Example of reconstruction of AWGN-affected greyscale images “Boat” ($\sigma = 25$) and “Barbara” ($\sigma = 35$) processed by sequential and parallel filtration schemes. In brackets PSNR, dB and MSSIM

TABLE 9
Average best results quality increase percentage
(for JPEG compressed 256×256 pixels images)

Q	PSNR	MSSIM
5	6.28%	6.33%
10	5.32%	3.58%
15	4.68%	1.80%

A greater number of tests held underlined some of the previously mentioned observations. It can be concluded that neither of the studied algorithms may be applied to the JPEG compressed images with $Q \geq 15$. Although they remove blocking artefacts from the input image each of them gives a decrease in MSSIM value of a reconstructed image. This decrease is expressed in smoothing too much detail from test images and in most cases is considered unacceptable.

TABLE 12
Algorithms comparison by the number of best results shown
(for JPEG compressed 512×512 pixels images)

Parameter	Q	APCA+Wiener	Sequential	Parallel
PSNR	5	7.00	1.00	8.00
MSSIM		8.00	1.45	6.55
PSNR	10	4.00	0.00	12.00
MSSIM		1.78	0.00	14.22
PSNR	15	1.00	0.00	15.00
MSSIM		0.94	0.00	15.06
Total		22.72	2.45	70.83
Total # tests		96		

TABLE 10
PSNR and MSSIM of JPEG compressed 512×512 pixels images after reconstruction

Image	Q	σ	Noised image		APCA+Wiener		Sequential scheme		Parallel scheme	
			PSNR, dB	MSSIM	PSNR, dB	MSSIM	PSNR, dB	MSSIM	PSNR, dB	MSSIM
Bridge	5	15	23.06	0.571	23.75	**0.597**	23.76	0.592	23.67	0.596
		20			**23.78**	0.589	23.75	0.576	23.76	0.591
		25			23.73	0.575	23.61	0.552	23.75	0.576
	10	15	25.13	0.711	25.66	0.713	25.54	0.698	**25.68**	**0.717**
		20			25.44	0.688	25.18	0.657	25.55	0.693
		25			25.09	0.656	24.65	0.609	25.21	0.657
	15	15	26.25	0.774	26.56	0.760	26.28	0.736	**26.65**	**0.766**
		20			26.11	0.724	25.67	0.682	26.30	0.729
		25			25.54	0.681	24.92	0.622	25.72	0.682
Barbara	5	15	23.86	0.664	25.03	0.723	25.10	0.724	24.86	0.718
		20			25.27	**0.728**	25.31	0.726	25.11	0.725
		25			**25.41**	0.727	25.40	0.723	25.31	0.727
	10	15	25.70	0.771	27.13	**0.814**	27.17	0.810	27.00	**0.814**
		20			**27.27**	0.808	27.17	0.796	27.19	0.809
		25			27.23	0.797	26.98	0.778	27.24	0.798
	15	15	27.05	0.822	28.61	0.853	28.60	0.846	28.53	**0.855**
		20			28.64	0.843	28.45	0.829	**28.67**	0.846
		25			28.42	0.829	28.02	0.807	28.57	0.831

TABLE 11
PSNR and MSSIM average increase rate of JPEG compressed 512×512 pixels images after reconstruction

Q	σ	PSNR			MSSIM		
		APCA+Wiener	Sequential	Parallel	APCA+Wiener	Sequential	Parallel
5	15	4.06%	**4.23%**	3.61%	**7.36%**	7.18%	6.93%
	20	4.51%	**4.55%**	4.31%	7.25%	6.40%	**7.32%**
	25	4.55%	4.31%	**4.61%**	5.16%	4.60%	**6.61%**
10	15	3.53%	3.28%	**3.65%**	2.59%	1.37%	**2.96%**
	20	2.94%	2.16%	**3.37%**	0.63%	-1.78%	**1.07%**
	25	1.90%	0.52%	**2.50%**	-1.85%	-5.38%	**-1.59%**
15	15	2.42%	1.70%	**2.76%**	0.21%	-1.65%	**0.67%**
	20	1.17%	-0.05%	**1.84%**	-2.43%	-5.23%	**-2.01%**
	25	-0.42%	-2.31%	**0.38%**	-5.44%	-9.51%	**-5.23%**

TABLE 13
Algorithms comparison by the percentage of best results shown
(for JPEG compressed 512×512 pixels images)

Parameter	Total # tests	APCA+Wiener	Sequential	Parallel
PSNR	48	25.00%	2.08%	72.92%
MSSIM	48	22.33%	3.03%	74.64%
Average		23.67%	2.56%	73.78%

TABLE 14
Average best results quality increase percentage
(for JPEG compressed 512×512 pixels images)

Q	PSNR	MSSIM
5	4.72%	7.84%
10	3.78%	2.79%
15	2.80%	0.67%

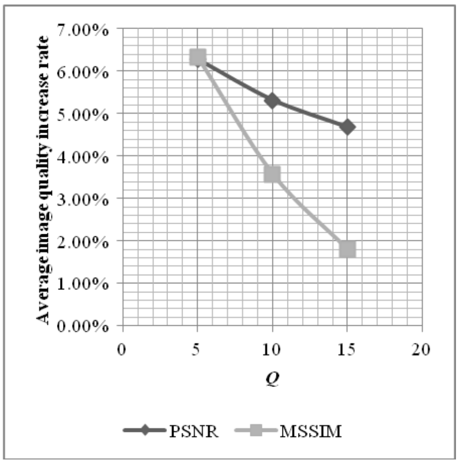

Fig. 5. Average PSNR and MSSIM increase rates for different Q values (for JPEG compressed 256×256 pixels images)

Applying sequential filtration scheme to a higher resolution images proved to be inadvisable because it showed lower average increase rates and it gave the least number of best reconstruction results both for PSNR and MSSIM. However comparing test results from Table 8 and Table 13 shows that APCA+Wiener filtration scheme which showed the minimum number of best results for 256×256 pixels images performed much better on 512×512 pixels images and its average quality increase rates given in Table 6 and Table 11 on average were better than the ones of sequential filtration scheme. This makes us consider the APCA+Wiener filtration method applicable for this task. On the other hand, parallel scheme strengthened its positions among the compared algorithms.

Results of JPEG compressed greyscale digital images filtration with the discussed filtration schemes are visualised on Fig. 7 on an example of "Scarlett" and "Pentagon" size of 512×512 pixels, and "Clock" and "Airplane" size of 256×256 pixels images.

It can be concluded that all the named filtration methods may be successfully applied to the task of removal of blocking artefacts with the notion to the listed limitations, however the reconstructed images quality shows to be relatively low and thus a further research in this area is needed.

B. AWGN-affected colour images filtration

The task is of especially current interest from the standpoint of modern applications. That is why numerous solutions were formulated to perform it. The one we used in the present work is a direct channelwise processing of an RGB image. For simplicity we did no transfer from RGB images to images with separated colour and brightness information [4]. AWGN was added to each channel independently with the same characteristics. Relevancy of use of the described noise model may be confirmed with the presence of image capture systems which consist of three separate CCDs or CMOS matrixes.

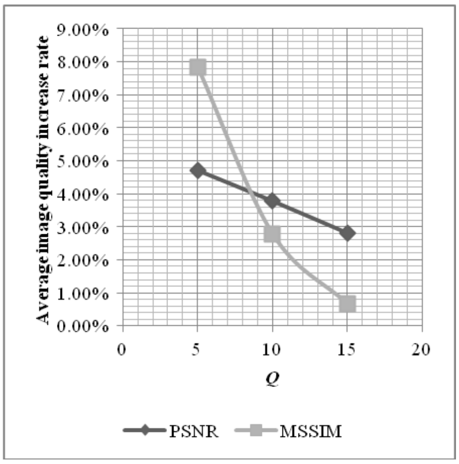

Fig. 6. Average PSNR and MSSIM increase rates for different Q values (for JPEG compressed 512×512 pixels images)

For this test we used 768×512 pixels colour images from the CIPR's Kodak image database [17]. We used AWGN with σ values in a range from 15 to 25.

Table 15 shows some numerical quality assessment results of noised image reconstruction on examples of "House" and "Door lock" images.

Average quality increase rate of PSNR and MSSIM values of a reconstructed image compared to an input AWGN-affected image for different σ values tested is shown in Table 16 for each of the studied schemes. The tendency of strong filtration quality results is observed for each scheme for all σ values tested, which justifies their applicability to this task.

Table 17 illustrates the algorithms comparison by the number of best results shown. Table 18 gives a percentile outlook of the same data. Notable is the fact that through our entire test series sequential scheme never showed a best performance neither in PSNR nor in MSSIM. This enforces our proposal of use the parallel filtration scheme with its approach of using two independent evaluations of an unnoised image $\mathbf{x}$. It should also be mentioned that

APCA+Wiener filtration scheme showed very competitive results in terms of MSSIM. This scheme even outperformed the parallel scheme for AWGN with $\sigma = 30$. That is why this scheme may be of use when a "good" instead of "excellent" colour images filtration results are needed.

TABLE 17
Algorithms comparison by the number of best results shown (for AWGN-affected colour images)

Parameter	σ	APCA+Wiener	Sequential	Parallel
PSNR	15	1.92	0.00	21.08
MSSIM		6.81	0.00	16.19
PSNR	20	1.00	0.00	22.00
MSSIM		9.00	0.00	14.00
PSNR	25	0.00	0.00	23.00
MSSIM		11.50	0.00	11.50
PSNR	30	0.00	0.00	23.00
MSSIM		12.46	0.00	10.54
PSNR	35	0.00	0.00	23.00
MSSIM		10.12	0.00	12.88
Total		52.81	0.00	177.19
Total # tests		230		

A final general overview of the proposed algorithms best performance results for this set of images is given in Table 19. It can be seen that growth in PSNR and MSSIM is almost linear, but as σ value of AWGN increases PSNR growth slows, and contrary, MSSIM growth fasters. This may be explained by our previously mentioned findings [8] – all the compared filtration methods provide a high-quality processing of main objects' edges. This fact shows its results in this test series – absolute values of PSNR and MSSIM decrease, but carefully processed edges slow this decrease for MSSIM.

Applying sequential filtration scheme to the task of colour images filtration proved to be infeasible as well as for the removal of blocking artefacts. At the same time parallel scheme showed almost absolute best performance for this task, especially according to PSNR quality assessment of reconstructed images.

Results of AWGN-affected colour digital images filtration with the named filtration schemes are visualised on Fig. 8 on examples of "Bikes", "Hibiscus", "Lighthouse", and "Child" images, all size of 768×512 pixels. Only fragments of high-resolution images are shown for easier comparing.

It can be concluded that APCA+Wiener and parallel filtration methods may be successfully applied to the task of AWGN-affected colour images filtration. Quality of the reconstructed images for these methods is rather high, although on high-resolution colour images the smoothing effect, which arises after filtration procedures, becomes more visible, due to the superposition of different image layer filtration defects. The smart way of layers integration may be of good help in solving the issue, and its implementation requires an additional study.

TABLE 19
Average best results quality increase percentage (for AWGN-affected colour images)

σ	PSNR	MSSIM
15	28.95%	38.15%
20	36.88%	61.48%
25	44.13%	86.84%
30	50.82%	113.47%
35	57.06%	141.37%

TABLE 15
PSNR and MSSIM of AWGN-affected colour images after reconstruction

Image	σ	Noised image		APCA+Wiener		Sequential scheme		Parallel scheme	
		PSNR, dB	MSSIM	PSNR, dB	MSSIM	PSNR, dB	MSSIM	PSNR, dB	MSSIM
House	15	24.64	0.797	28.97	0.873	28.20	0.838	**29.11**	**0.879**
	20	22.17	0.713	27.46	0.820	27.03	0.788	**27.74**	**0.827**
	25	20.27	0.638	26.36	0.771	26.10	0.740	**26.67**	**0.775**
	30	18.74	0.572	25.51	**0.726**	25.32	0.695	**25.77**	0.725
	35	17.45	0.515	24.80	**0.684**	24.64	0.652	**25.01**	0.678
Door lock	15	24.75	0.566	32.70	**0.849**	32.38	0.834	**32.82**	0.847
	20	22.37	0.443	31.51	**0.818**	31.29	0.804	**31.63**	0.814
	25	20.57	0.355	30.58	**0.793**	30.41	0.780	**30.70**	0.789
	30	19.12	0.292	29.78	**0.773**	29.63	0.760	**29.90**	0.769
	35	17.91	0.245	29.03	**0.757**	28.90	0.745	**29.16**	0.753


a) Noised image “Scarlett” (28.66 dB; 0.732)


b) APCA+Wiener (30.90 dB; 0.821)

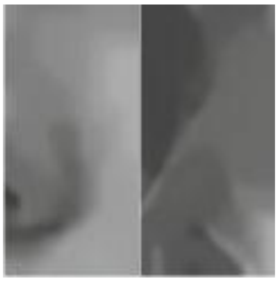
c) Sequential scheme (30.83 dB; 0.818)

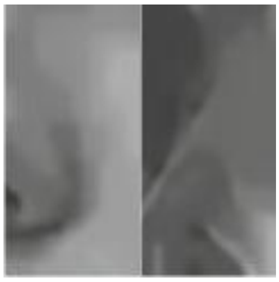
d) Parallel scheme (30.86 dB; 0.820)


e) Noised image “Clock” (28.77 dB; 0.879)


f) APCA+Wiener (29.74 dB; 0.912)


g) Sequential scheme (29.68 dB; 0.912)


h) Parallel scheme (29.86 dB; 0.915)


i) Noised image “Pentagon” (25.17 dB; 0.615)

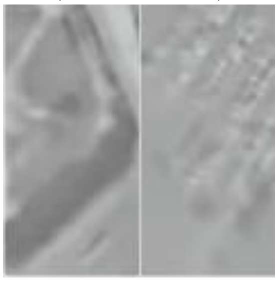
j) APCA+Wiener (25.21 dB; 0.575)

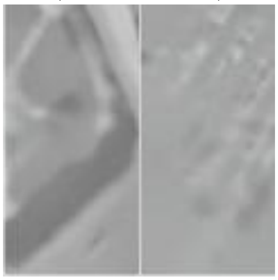
k) Sequential scheme (24.89 dB; 0.544)

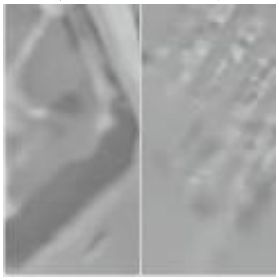
l) Parallel scheme (25.31 dB; 0.579)


m) Noised image “Airplane” (28.1 dB; 0.813)


n) APCA+Wiener (29.57 dB; 0.874)


o) Sequential scheme (29.64 dB; 0.878)


p) Parallel scheme (29.33 dB; 0.868)

Fig. 7. Example of reconstruction of JPEG compressed greyscale images “Scarlett” ($Q = 5$, $\sigma = 25$), “Clock” ($Q = 10$, $\sigma = 20$), “Pentagon” ($Q = 10$, $\sigma = 25$), and “Airplane” ($Q = 5$, $\sigma = 15$) processed by APCA+Wiener, sequential and parallel filtration schemes. In brackets PSNR, dB and MSSIM

TABLE 16
PSNR and MSSIM average increase rate of AWGN-affected colour images after reconstruction

σ	PSNR			MSSIM		
	APCA+Wiener	Sequential	Parallel	APCA+Wiener	Sequential	Parallel
15	28.34%	24.34%	**28.89%**	37.73%	35.30%	**38.09%**
20	35.77%	34.32%	**36.86%**	60.99%	58.14%	**61.27%**
25	42.70%	41.66%	**44.13%**	86.26%	82.92%	**86.46%**
30	49.21%	48.37%	**50.82%**	112.89%	108.98%	**112.91%**
35	55.34%	54.60%	**57.06%**	**140.66%**	136.27%	140.60%

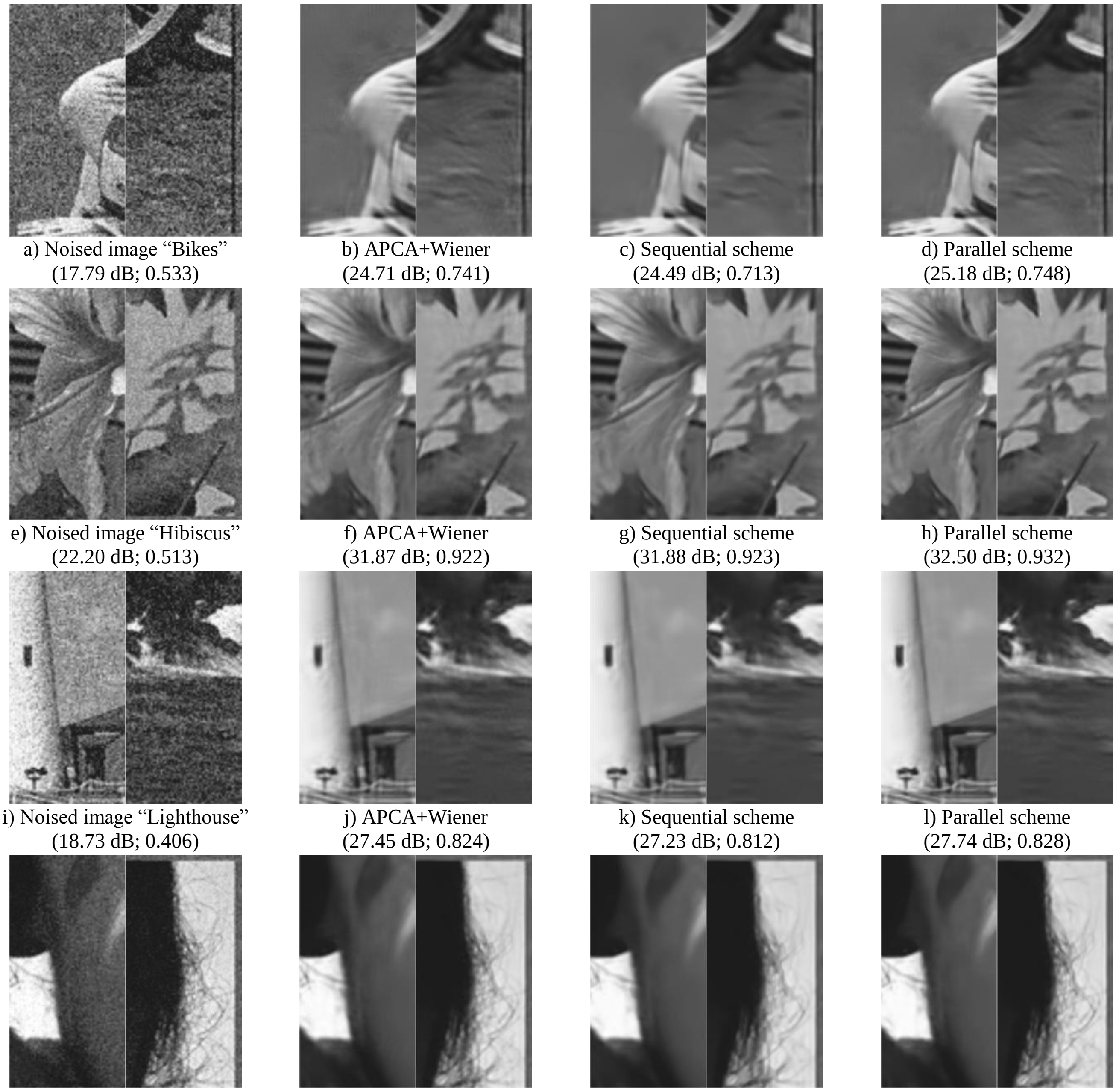

a) Noised image “Bikes” (17.79 dB; 0.533)
b) APCA+Wiener (24.71 dB; 0.741)
c) Sequential scheme (24.49 dB; 0.713)
d) Parallel scheme (25.18 dB; 0.748)
e) Noised image “Hibiscus” (22.20 dB; 0.513)
f) APCA+Wiener (31.87 dB; 0.922)
g) Sequential scheme (31.88 dB; 0.923)
h) Parallel scheme (32.50 dB; 0.932)
i) Noised image “Lighthouse” (18.73 dB; 0.406)
j) APCA+Wiener (27.45 dB; 0.824)
k) Sequential scheme (27.23 dB; 0.812)
l) Parallel scheme (27.74 dB; 0.828)
m) Noised image “Child” (24.96 dB; 0.599)
n) APCA+Wiener (32.93 dB; 0.889)
o) Sequential scheme (32.46 dB; 0.875)
p) Parallel scheme (33.05 dB; 0.890)

Fig. 8. Example of reconstruction of AWGN-affected colour images “Bikes” ($\sigma = 35$), “Hibiscus” ($\sigma = 20$), “Lighthouse” ($\sigma = 30$), and “Child” ($\sigma = 15$) processed by APCA+Wiener, sequential and parallel filtration schemes. In brackets PSNR, dB and MSSIM

TABLE 18
Algorithms comparison by the percentage of best results shown (for AWGN-affected colour images)

Parameter	Total # tests	APCA+Wiener	Sequential	Parallel
PSNR	115	2.54%	0.00%	97.46%
MSSIM	115	43.39%	0.00%	56.61%
Average		22.96%	0.00%	77.04%

C. *Mixed noise images filtration*

The discussed AWGN model may be complicated by a usage of mixed noise model. An example of such model was proposed by Hirakawa and Parks in 2006 [18] to characterize noise of CMOS matrixes. The model may be described as follows:

$$\mathbf{y} = \mathbf{x} + (\sigma_1 + \sigma_2 \mathbf{x})\mathbf{n}, \quad (6)$$

where σ_1 and σ_2 – are the constants which determine a noisiness degree, and $\mathbf{n}$ – is an AWGN with zero mean and $\sigma = 1$. If $\sigma_2 = 0$ this noise model becomes the described earlier AWGN model.

Because of the irregular character of noise dispersion in the mixed noise model, which is explained by the dependency of noise from the initial signal, a direct application of the described schemes is impossible. For this reason we used a generalized homomorphic filtration method [19], proposed by Ding and Venetsanopoulos in 1987. The idea of this method is in using a logarithm-type transform to interpret noised data $\mathbf{y}$ as a sum of an initial unnoised signal and AWGN, process them with described filtration schemes and then reconstruct the data with the inverse transform.

For this test we used all the mentioned above images – 256×256 and 512×512 pixels greyscale and 768×512 pixels colour images from [14, 17]. We used a mixed noise with σ_1 values in a range from 15 to 25 and σ_2 values in a range from 0.1 to 0.3.

Table 20 shows some numerical quality assessment results of noised image reconstruction on examples of "Chemical Plant" size of 256×256 greyscale image, "Terminal" size of 512×512 greyscale image and "House" size of 768×512 colour image.

Average quality increase rate of PSNR and MSSIM values of a reconstructed image compared to an input mixed noise affected image for different σ_1 and σ_2 values tested are shown in: Table 21 for 256×256 greyscale images, Table 22 for 512×512 greyscale images and Table 23 for 768×512 colour images, for each of the studied schemes. The tendency of strong filtration quality results is observed for each scheme for all σ_1 and σ_2 values tested, which as well justifies their applicability to this task.

The algorithms comparisons by the number of best results are given in: Table 24 for 256×256 greyscale images, Table 25 for 512×512 greyscale images and Table 26 for 768×512 colour images. Tables 27, 28 and 29 give a percentile outlook of the same data. It can be observed that the parallel filtration scheme showed best results of image reconstruction on a PSNR scale in a prevailing number of tests. However, MSSIM quality assessment results were almost equally distributed between all three filtration schemes. This may be explained by the fact that the MSSIM values are formed based on evaluating the image, which colour layers were processed independently, so that each scheme at the end formed a synergetic reconstructed image. This is why in Tables 21, 22, and 23 a dramatic MSSIM values increase is observed.

A final general overview of the proposed algorithms best performance results is given in: Table 30 for 256×256 greyscale images, Table 31 for 512×512 greyscale images and Table 32 for 768×512 colour images. Similar to the notes which were made for the AWGN-affected images filtration may be made for this test. PSNR and MSSIM increase for correlating pairs of results is almost linear. All the compared filtration methods provide a high-quality processing of main objects' edges and filtration quality in general.

Although sequential filtration scheme showed nearly as many best results as parallel scheme on MSSIM scale for 256×256 pixels greyscale images, application of the sequential filtration scheme to this task is infeasible for the higher resolution images and colour images. At the same time parallel scheme showed almost absolute best performance in this task, especially according to PSNR quality assessment of reconstructed images.

TABLE 30
Average best results quality increase percentage
(for mixed noise affected 256×256 pixels greyscale images)

σ_1	σ_2	PSNR	MSSIM
15	0.1	43.14%	176.89%
	0.2	49.88%	287.64%
	0.3	50.88%	389.89%
20	0.1	47.88%	213.61%
	0.2	53.22%	328.26%
	0.3	53.94%	435.89%
25	0.1	52.11%	250.84%
	0.2	56.49%	368.68%
	0.3	56.62%	481.10%

TABLE 31
Average best results quality increase percentage
(for mixed noise affected 512×512 pixels greyscale images)

σ_1	σ_2	PSNR	MSSIM
15	0.1	45.51%	132.84%
	0.2	57.32%	212.84%
	0.3	61.33%	285.79%
20	0.1	52.10%	175.19%
	0.2	62.31%	260.58%
	0.3	65.35%	340.93%
25	0.1	58.28%	219.18%
	0.2	67.00%	309.46%
	0.3	69.16%	394.69%

TABLE 32
Average best results quality increase percentage
(for mixed noise affected 768×512 pixels colour images)

σ_1	σ_2	PSNR	MSSIM
15	0.1	42.14%	84.00%
	0.2	52.12%	135.54%
	0.3	56.09%	183.35%
20	0.1	48.38%	109.22%
	0.2	57.18%	162.24%
	0.3	60.37%	211.10%
25	0.1	54.23%	134.77%
	0.2	61.97%	188.61%
	0.3	64.38%	239.65%

Results of mixed noise affected greyscale and colour digital images filtration with the discussed filtration schemes are visualised on Fig. 9 on examples of "Clock" 256×256 pixels greyscale image with ($\sigma_1=25$, $\sigma_2=0.1$), "Village" 512×512 pixels greyscale image with ($\sigma_1=20$, $\sigma_2=0.3$) and "Lady" 768×512 pixels colour image with ($\sigma_1=15$, $\sigma_2=0.1$). Only fragments of the images are shown for easier comparing.

Application of all three algorithms to images affected by this noise model on high levels of σ_1 and σ_2 resulted in visible colour changes of minor image details and objects. For example, on a "Caps" colour image several little clouds previously of a white colour were reconstructed as red-like, because of the high number of red noise pixels on an input noised image. We consider this type of reconstruction defects significant as they are easily noticeable, and we understand that for a successful use of the discussed filtration schemes to the mixed noise filtration on colour images some additions to the algorithms need to be made. However the overall quality of reconstructed images which were noised with $\sigma_2 = \{0.1, 0.2\}$ is high and the defects described above are unnoticeable. That is why it can be concluded that APCA+Wiener and parallel filtration methods may be successfully applied to the task of mixed noise affected greyscale and colour images filtration with limitation in using the high σ_2 values for colour images.

TABLE 20
PSNR and MSSIM of various resolution mixed noise affected images after reconstruction

Image	σ_1	σ_2	Noised image		APCA+Wiener		Sequential scheme		Parallel scheme	
			PSNR, dB	MSSIM	PSNR, dB	MSSIM	PSNR, dB	MSSIM	PSNR, dB	MSSIM
House (256×256)	15	0.1	19.90	0.623	26.10	0.766	25.89	0.736	**26.42**	**0.768**
		0.2	16.86	0.490	24.15	**0.683**	24.13	0.659	**24.47**	0.678
		0.3	14.76	0.395	22.27	**0.612**	22.35	0.598	**22.63**	0.605
	20	0.1	18.42	0.557	25.30	**0.722**	25.16	0.693	**25.59**	0.720
		0.2	15.86	0.442	23.60	**0.645**	23.57	0.619	**23.87**	0.635
		0.3	14.05	0.361	21.92	**0.577**	21.96	0.558	**22.18**	0.564
	25	0.1	17.18	0.500	24.64	**0.681**	24.51	0.650	**24.88**	0.674
		0.2	14.99	0.401	23.12	**0.607**	23.06	0.577	**23.33**	0.593
		0.3	13.43	0.331	21.59	**0.542**	21.56	0.515	**21.76**	0.525
Chemical Plant (512×512)	15	0.1	19.96	0.462	27.16	0.786	26.90	0.773	**27.28**	**0.789**
		0.2	16.97	0.334	24.86	0.709	24.83	0.704	**25.12**	**0.716**
		0.3	14.89	0.252	22.61	0.629	22.72	0.635	**22.91**	**0.640**
	20	0.1	18.47	0.392	26.32	0.751	26.15	0.738	**26.51**	**0.754**
		0.2	15.96	0.289	24.27	0.679	24.25	0.672	**24.50**	**0.683**
		0.3	14.16	0.223	22.26	0.607	22.31	0.608	**22.48**	**0.611**
	25	0.1	17.22	0.337	25.61	0.718	25.49	0.705	**25.83**	**0.721**
		0.2	15.08	0.253	23.75	**0.651**	23.71	0.640	**23.94**	**0.651**
		0.3	13.53	0.199	21.91	**0.583**	21.88	0.575	**22.06**	0.582
Terminal (768×512)	15	0.1	20.73	0.478	25.76	0.682	25.32	0.650	**26.00**	**0.683**
		0.2	18.07	0.362	24.10	**0.611**	23.91	0.588	**24.29**	0.610
		0.3	16.14	0.283	22.63	**0.553**	22.57	0.539	**22.76**	0.549
	20	0.1	19.12	0.404	25.01	**0.642**	24.71	0.614	**25.23**	**0.642**
		0.2	16.93	0.312	23.61	**0.579**	23.45	0.556	**23.73**	0.574
		0.3	15.29	0.248	22.29	**0.524**	22.21	0.506	**22.34**	0.515
	25	0.1	17.80	0.346	24.42	**0.607**	24.19	0.581	**24.59**	0.604
		0.2	15.96	0.272	23.18	**0.548**	23.02	0.524	**23.24**	0.539
		0.3	14.56	0.220	**21.99**	**0.496**	21.85	0.471	21.98	0.483

TABLE 21
PSNR and MSSIM average increase rate of mixed noise affected 256×256 pixels greyscale images after reconstruction

σ_1	σ_2	PSNR			MSSIM		
		APCA+Wiener	Sequential	Parallel	APCA+Wiener	Sequential	Parallel
15	0.1	35.74%	36.00%	**37.41%**	171.38%	174.97%	**175.70%**
	0.2	47.27%	48.08%	**49.68%**	239.60%	**250.24%**	249.30%
	0.3	42.04%	21.00%	**44.51%**	305.13%	273.47%	**332.46%**
20	0.1	39.62%	39.96%	**41.63%**	181.20%	185.00%	**185.98%**
	0.2	44.34%	44.95%	**46.57%**	274.71%	**285.87%**	284.72%
	0.3	44.87%	22.69%	**47.20%**	348.51%	303.88%	**372.97%**
25	0.1	43.18%	43.56%	**45.44%**	212.97%	217.39%	**218.55%**
	0.2	47.16%	47.65%	**49.43%**	310.08%	**321.09%**	320.25%
	0.3	47.39%	47.88%	**49.54%**	392.73%	**418.92%**	412.93%

TABLE 22

PSNR and MSSIM average increase rate of mixed noise affected 512×512 pixels greyscale images after reconstruction

σ_1	σ_2	PSNR			MSSIM		
		APCA+Wiener	Sequential	Parallel	APCA+Wiener	Sequential	Parallel
15	0.1	44.26%	43.68%	**45.51%**	131.12%	129.19%	**132.64%**
	0.2	55.37%	55.62%	**57.32%**	207.00%	210.18%	**212.00%**
	0.3	58.62%	38.70%	**61.33%**	265.93%	241.01%	**284.01%**
20	0.1	50.66%	50.28%	**52.10%**	172.85%	171.09%	**174.70%**
	0.2	60.44%	60.65%	**62.31%**	253.53%	257.34%	**259.06%**
	0.3	63.18%	42.31%	**65.35%**	320.34%	292.82%	**336.57%**
25	0.1	56.77%	56.43%	**58.27%**	216.06%	214.38%	**218.18%**
	0.2	65.27%	65.29%	**67.00%**	301.63%	305.11%	**307.08%**
	0.3	67.39%	67.72%	**69.15%**	376.63%	**392.11%**	389.78%

TABLE 23

PSNR and MSSIM average increase rate of mixed noise affected 768×512 pixels colour images after reconstruction

σ_1	σ_2	PSNR			MSSIM		
		APCA+Wiener	Sequential	Parallel	APCA+Wiener	Sequential	Parallel
15	0.1	44.36%	43.91%	**46.36%**	82.94%	80.97%	**83.83%**
	0.2	49.75%	50.12%	**52.12%**	132.63%	132.71%	**135.14%**
	0.3	53.19%	52.71%	**56.09%**	173.79%	176.40%	**183.12%**
20	0.1	46.39%	46.11%	**48.38%**	107.95%	105.73%	**108.92%**
	0.2	54.92%	55.22%	**57.18%**	158.94%	158.92%	**161.59%**
	0.3	57.98%	57.92%	**60.37%**	202.70%	206.42%	**210.45%**
25	0.1	52.20%	51.95%	**54.23%**	133.41%	130.73%	**134.26%**
	0.2	59.88%	60.00%	**61.97%**	185.52%	184.79%	**187.70%**
	0.3	68.69%	69.09%	**70.81%**	232.18%	236.59%	**237.75%**

TABLE 24

Algorithms comparison by the number of best results shown

(for mixed noise affected 256×256 pixels greyscale images)

σ_1	σ_2	APCA+Wiener		Sequential		Parallel	
		PSNR	MSSIM	PSNR	MSSIM	PSNR	MSSIM
15	0.1	0.00	1.00	1.00	3.00	6.00	3.00
	0.2	0.00	0.00	1.00	4.00	6.00	3.00
	0.3	0.00	0.00	1.00	3.00	6.00	4.00
20	0.1	0.00	1.00	1.00	3.00	6.00	3.00
	0.2	0.00	0.00	0.00	3.50	7.00	3.50
	0.3	0.00	0.00	0.00	3.50	7.00	3.50
25	0.1	0.00	1.00	1.00	3.00	6.00	3.00
	0.2	0.00	0.80	0.00	2.63	7.00	3.58
	0.3	0.00	2.00	0.00	3.00	7.00	2.00
Total		5.80		33.63		86.58	
Total # tests		126					

TABLE 27

Algorithms comparison by the percentage of best results shown

(for mixed noise affected 256×256 pixels greyscale images)

Parameter	Total # tests	APCA+Wiener	Sequential	Parallel
PSNR	63	0.00%	7.94%	92.06%
MSSIM	63	9.21%	45.44%	45.36%
Average		4.60%	26.69%	68.71%

TABLE 25
Algorithms comparison by the number of best results shown
(for mixed noise affected 512×512 pixels greyscale images)

σ_1	σ_2	APCA+Wiener		Sequential		Parallel	
		PSNR	MSSIM	PSNR	MSSIM	PSNR	MSSIM
15	0.1	0.00	2.82	0.00	0.00	16.00	13.18
	0.2	0.00	6.00	0.00	3.33	16.00	6.67
	0.3	0.00	3.00	0.00	6.00	16.00	7.00
20	0.1	0.00	4.71	0.00	0.00	16.00	11.29
	0.2	0.00	6.00	0.00	3.00	16.00	7.00
	0.3	0.00	4.00	0.00	9.00	16.00	3.00
25	0.1	1.00	6.00	0.00	0.00	15.00	10.00
	0.2	0.00	6.00	0.00	3.00	16.00	7.00
	0.3	1.00	5.00	0.00	7.62	15.00	3.38
Total		45.53		31.95		210.52	
Total # tests		288					

TABLE 26
Algorithms comparison by the number of best results shown
(for mixed noise affected 768×512 pixels colour images)

σ_1	σ_2	APCA+Wiener		Sequential		Parallel	
		PSNR	MSSIM	PSNR	MSSIM	PSNR	MSSIM
15	0.1	0.00	4.00	0.00	0.00	10.00	6.00
	0.2	0.00	2.00	0.00	1.00	10.00	7.00
	0.3	0.00	1.00	0.00	0.00	10.00	9.00
20	0.1	0.00	3.00	0.00	0.00	10.00	7.00
	0.2	0.00	2.00	0.00	1.00	10.00	7.00
	0.3	0.00	1.00	0.00	1.00	10.00	8.00
25	0.1	0.00	3.00	0.00	0.00	10.00	7.00
	0.2	0.00	2.00	0.00	1.00	10.00	7.00
	0.3	0.00	1.00	0.00	3.00	10.00	6.00
Total		19.00		7.00		154.00	
Total # tests		180					

TABLE 28
Algorithms comparison by the percentage of best results shown
(for mixed noise affected 512×512 pixels greyscale images)

Parameter	Total # tests	APCA+Wiener	Sequential	Parallel
PSNR	144	1.39%	0.00%	98.61%
MSSIM	144	30.23%	22.19%	47.58%
Average		15.81%	11.09%	73.10%

TABLE 29
Algorithms comparison by the percentage of best results shown
(for mixed noise affected 768×512 pixels colour images)

Parameter	Total # tests	APCA+Wiener	Sequential	Parallel
PSNR	90	0.00%	0.00%	100.00%
MSSIM	90	21.11%	7.78%	71.11%
Average		10.56%	3.89%	85.56%

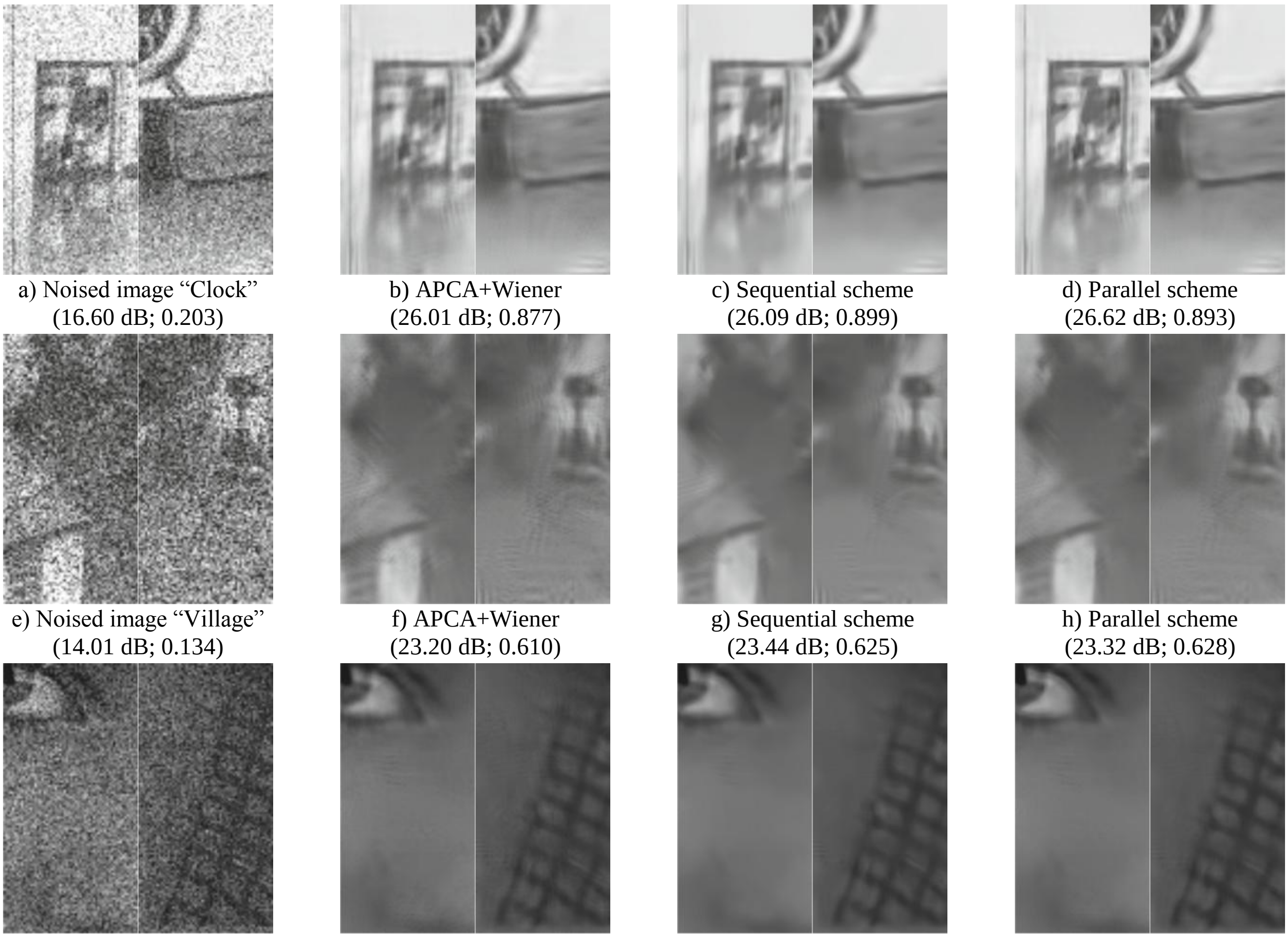

a) Noised image “Clock” (16.60 dB; 0.203)
b) APCA+Wiener (26.01 dB; 0.877)
c) Sequential scheme (26.09 dB; 0.899)
d) Parallel scheme (26.62 dB; 0.893)
e) Noised image “Village” (14.01 dB; 0.134)
f) APCA+Wiener (23.20 dB; 0.610)
g) Sequential scheme (23.44 dB; 0.625)
h) Parallel scheme (23.32 dB; 0.628)
i) Noised image “Lady” (17.24 dB; 0.293)
j) APCA+Wiener (28.06 dB; 0.773)
k) Sequential scheme (28.14 dB; 0.772)
l) Parallel scheme (28.39 dB; 0.777)

Fig. 9. Example of reconstruction of mixed noise affected images: “Clock” ($\sigma_1 = 25$, $\sigma_2 = 0.1$), “Village” ($\sigma_1 = 20$, $\sigma_2 = 0.3$), and “Lady” ($\sigma_1 = 15$, $\sigma_2 = 0.2$) processed by APCA+Wiener, sequential and parallel filtration schemes. In brackets PSNR, dB and MSSIM

V. COMPUTATIONAL COSTS

Although we have already discussed the computational costs of the parallel filtration scheme [8], in the present work we would like to compare the computational costs of the used algorithms in order to give a complete coverage of the question of their applicability to the abovementioned digital image processing tasks.

Consider N and M – number of strings and columns of a processed image, respectfully, ΔN – step in pixels, which a denoise region is moved on, n – number of training vectors found in a train regions, m – length of training vectors, depicted as column-vectors, l – parameter, setting up a size of similarity area, and g – parameter, setting up a size of similar pixels search area.

A. Modification of the two-stage PCA filtration algorithm

Calculations connected with creation of covariation matrix, search for eigenvectors (principal components) and data interpretation in a found principal components’ basis require $O(nm^2)$ operations for each denoise region.

Data transform coefficients computation, shown in the found principal components’ basis, performed using LMMSE estimator during the first stage and using empirical Wiener filter during the second stage, combined require $O(nm)$ operations for each denoise region.

Therefore, the APCA+Wiener filtration scheme has computation costs of:

$$O\left[\frac{NM}{\Delta N}\cdot\left(O(nm^2)+O(nm)\right)\right], \quad (7)$$

there $\frac{NM}{\Delta N}$ represents the number of denoise regions per processed image.

B. Sequential filtration scheme

Sequential scheme uses a third processing stage based on non-local processing algorithm which requires $O(NMl^2g^2)$ operations in total. As you can see this component is highly dependable on the parameters algorithm uses, but in general it drastically increases the total run time of the filtration algorithm compared to the APCA+Wiener.

Total computational costs of the three staged sequential filtration scheme are as follows:

$$O\left[\frac{NM}{\Delta N}\cdot\left(O(nm^2)+O(nm)\right)\right]+O(NMl^2g^2)\,. \quad (8)$$

C. Parallel filtration scheme

Its difference from the sequential scheme in a computational costs sense is in addition of a fourth stage of mixing pixels. This procedure requires as low as $O(NM)$ operations in total.

A resulting equation describing the computation cost of the proposed algorithm:

$$O\left[\frac{NM}{\Delta N}\cdot\left(O(nm^2)+O(nm)\right)\right]+O(NMl^2g^2)+O(NM). \quad (9)$$

An addition of the fourth stage does not give any significant run time increase, because, as it was mentioned above, third processing stage – "Non-local algorithm of image filtration" comprises the most of the total computational costs.

As we stated before computation costs of the sequential and parallel scheme algorithms are relatively high in comparison with APCA+Wiener and other existed denoising algorithms. There are several possible approaches which can be used to decrease the cost: (1) calculate only first largest eigenvalues and correspondent eigenvectors for creation of principal components' basis [20]; (2) during the processing of a noised image change a procedure of searching a local principal component basis with a creation of global hierarchical principal component basis [21]; (3) while using a non-local processing algorithm [6, 9-11] implement it in a vector form [9,10], or, alternatively, use a global principal components' basis separately calculated for a processed image – this will reduce size of compared similarity areas of pixels being processed and analyzed, and speed up calculation of weight coefficients used to form a final evaluation of an unnoised pixel [22].

With these steps taken we believe the described algorithms will perform using less computational resources. They surely will not be close to the APCA+Wiener performance but their use will be more flexible. For example, if APCA+Wiener algorithm implemented using a lower level than MATLAB programming language may be used for video stream, sequential and parallel schemes will still most likely be applicable only for separate images processing.

VI. Comparison of the used filtration methods

Here we give a brief discussion on the filtration schemes performance in the described digital image processing applications.

A. *Modification of the two-stage PCA filtration scheme*

The most advantageous feature of this method is its low computational cost and construction simplicity.

Primary disadvantages of using this filtration scheme from the standpoint of reconstructed images quality are: (1) substantial amount of ringing artefacts on image objects' edges, this effect is especially visible on high-contrast image parts (for example see Fig. 8, b) and f)); (2) high blurring of image objects' edges, compared to other modern filtration methods [3-5].

According to the application tests performed APCA+Wiener filtration scheme showed good results in: (1) removal of blocking artefacts from 512×512 pixels greyscale images; (2) AWGN-affected colour images filtration; (3) mixed noise affected 512×512 pixels greyscale and 768×512 pixels colour images filtration. These good results were achieved mostly due to the high MSSIM values; PSNR results shown by this filtration scheme are modest in all tests, except of the removal of blocking artefacts from 512×512 pixels greyscale images (see Table 13).

B. *Sequential filtration scheme*

Advantages of this method are in its relative construction and implementation simplicity and the decrease of the amount of ringing artefacts on image objects' edges (for example see Fig. 8, c) and g)).

Primary disadvantages of using this filtration scheme are in the presence of high blurring of image objects' edges and high computational cost of the filtration algorithm.

According to the application tests performed sequential filtration scheme showed good results in: (1) removal of blocking artefacts from 256×256 pixels greyscale images; (2) mixed noise affected 256×256 pixels and 512×512 pixels greyscale images filtration. Similarly to the APCA+Wiener, these good results were achieved mostly due to the high MSSIM values; PSNR results shown by this filtration scheme are modest in all tests, except the removal of blocking artefacts from 256×256 pixels greyscale images (see Table 8).

C. *Parallel filtration scheme*

Advantages of this method are: (1) high quality of the reconstructed images both on PSNR and MSSIM scales; (2) minimal amount of ringing artefacts on image objects' edges, and low blurring of image objects' edges (for example see Fig. 8, d) and h)).

Primary disadvantage of using this filtration scheme is in the high computational cost of the filtration algorithm.

In all tests held the parallel filtration scheme showed nearly absolute best performance on PSNR scale and significantly outperformed its competitors on MSSIM scale. However in the task of blocking artefacts removal from 256×256 pixels greyscale images on MSSIM scale its lead from two other algorithms was less than 10% (see Table 8) and less than 15% in the task of AWGN-affected 768×512 pixels colour images filtration (see Table 18).

VII. Conclusion

Our study has shown how different digital image filtration algorithms based on the PCA and non-local processing may be applied to modern digital image processing tasks. Experimental results obtained prove the idea of successful application of these filtration methods to the removal of blocking artefacts, AWGN- and mixed noise affected image filtration. In the present work we listed the limitations of use for each method and proposed approaches of their overcome.

Our further research will unveil the implementation results of the mentioned approaches and some other possible applications of the discussed filtration methods.

References

[1] Chatterjee P., Milanfar P. Is denoising dead? *IEEE Trans. Image Processing*. 2010. V. 19, №4. pp. 895–911.

[2] Katkovnik V., Foi A., Egiazarian K., Astola J. From local kernel to nonlocal multiple-model image denoising, *Int. J. Computer Vision*. 2010. V. 86, №8. pp. 1–32.

[3] Dabov K., Foi A., Katkovnik V., Egiazarian K. Image denoising by sparse 3D transform-domain collaborative filtering, *IEEE Trans. Image Processing*. 2007. V. 16, №8. pp. 2080–2095.

[4] Foi A., Katkovnik V., Egiazarian K. Pointwise shape-adaptive DCT for high-quality denoising and deblocking of grayscale and color images, *IEEE Trans. Image Processing*. 2007. V. 16, №5. pp. 1395-1411.

[5] Aharon M., Elad M., Bruckstein A., Katz Y. The K-SVD: An algorithm for designing of overcomplete dictionaries for sparse representation, *IEEE Trans. Signal Processing*. 2006. V. 54, №11. pp. 4311–4322.

[6] Buades A., Coll B., Morel J.M. A non-local algorithm for image denoising, *Proc. IEEE Comp. Soc. Conf. Computer Vision and Pattern Recognition*. 2005. V. 2. pp. 60–65.

[7] Katkovnik V., Foi A., Egiazarian K., Astola J. Directional varying scale approximations for anisotropic signal processing, Proc. XII *European Signal Processing Conf*. 2004. pp. 101–104.

[8] Priorov A., Volokhov V., Sergeev E., Mochalov I., Tumanov K. *Parallel filtration based on Principle Component Analysis and nonlocal image processing*, Lecture Notes in Engineering and Computer Science: Proc. Int. MultiConf. of Engineers and Computer Scientists 2013, 13-15 March, 2013, Hong Kong, pp. 430-435.

[9] Buades A., Coll B., Morel J.M. A review of image denoising algorithms, with a new one, *Multiscale Modeling and Simulation: A SIAM Interdisciplinary Journal*. 2005. V. 4. pp. 490–530.

[10] Buades A. Image and film denoising by non-local means. *PhD thesis*, Universitat de les Illes Balears. 2005.

[11] Buades A., Coll B., Morel J.M. Nonlocal image and movie denoising, *Int. J. Computer Vision*. 2008. V. 76, №2. pp. 123–139.

[12] Salomon D. Data, image and audio compression, *Technoshere.* 2004.

[13] Wang Z., Bovik A.C., Sheikh H.R., Simoncelli E.P. Image quality assessment: from error visibility to structural similarity, *IEEE Trans. Image Processing*. 2004. V. 13, №4. pp. 600–612.

[14] University of Granada Computer Vision Group test images database, http://decsai.ugr.es/cvg/dbimagenes. 2013

[15] Salomon D. A guide to data compression methods, *Springer*. 2002.

[16] Gonsales R., Woods R. Digital image processing, *Prentice Hall*. 2008.

[17] The RPI-CIPR Kodak image database, http://www.cipr.rpi.edu/resource/stills/kodak.html. 2013

[18] Hirakawa K., Parks T.W. Image denoising using total least squares, *IEEE Trans. Image Processing*. 2006. V. 15, №9. pp. 2730-2742.

[19] Ding R., Venetsanopoulos A.N. Generalized homomorphic and adaptive order statistic filters for the removal of impulsive and signal-dependent noise, *IEEE Trans. Circuits Syst.* 1987. V. CAS–34, №8. pp. 948–955.

[20] Du Q., Fowler J.E. Low-complexity principal component analysis for hyperspectral image compression, *Int. J. High Performance Computing Applications*. 2008. V. 22. pp. 438–448.

[21] Deledalle C.-A., Salmon J., Dalalyan A. Image denoising with patch based PCA: local versus global, *Proc. 22nd British Machine Vision Conf.* 2011. pp. 25.1-25.10

[22] Tasdizen T. Principal components for non-local means image denoising, *Proc. IEEE Int. Conf. Image Processing*. 2008. pp. 1728-1731.